Mapping the Binding Site for Matrix Metalloproteinase on the N-Terminal Domain of the Tissue Inhibitor of Metalloproteinases-2 by NMR Chemical Shift Perturbation†

Richard A. Williamson,*,‡ Mark D. Carr,*,‡ Tom A. Frenkiel,§ James Feeney,|| and Robert B. Freedman‡

Research School of Biosciences, University of Kent, Canterbury, Kent CT2 7NJ, U.K., and MRC Biomedical NMR Centre and Division of Molecular Structure, National Institute for Medical Research, The Ridgeway, Mill Hill, London NW7 1AA, U.K.

Received May 22, 1997; Revised Manuscript Received August 4, 1997⊗

ABSTRACT: Changes in the NMR chemical shift of backbone amide nuclei (^{1}H and ^{15}N) have been used to map the matrix metalloproteinase (MMP) binding site on the N-terminal domain of *the* tissue inhibitor of metalloproteinase-2 (N-TIMP-2). Amide chemical shift changes were measured on formation of a stable complex with the catalytic domain of stromelysin-1 (N-MMP-3). Residues with significantly shifted amide signals mapped specifically to a broad site covering one face of the molecule. This site (the MMP binding site) consists primarily of residues 1−11, 27−41, 68−73, 87−90, and 97−104. The site overlaps with the OB-fold binding site seen in other proteins that share the same five-stranded β-barrel topology. Sequence conservation data and recent site-directed mutagenesis studies are discussed in relation to the MMP binding site identified in this work.

Breakdown of the extracellular matrix is an important event in many normal and pathological processes, such as growth, wound healing, tumor invasion, and rheumatoid and osteoarthritis. The matrix metalloproteinases (MMPs)[1] are a family of zinc endopeptidases thought to be primarily responsible for extracellular matrix catabolism (Woessner, 1991; Docherty *et al*., 1992). The activity of these enzymes is highly regulated, and a key mechanism of regulation includes a family of specific inhibitors, the tissue inhibitors of metalloproteinases (TIMPs), which form tight (K_d < 1 nM), 1:1 noncovalent complexes with the active enzymes (Murphy & Willenbrock, 1995). Four TIMPs have now been identified (Docherty *et al*., 1985; Boone *et al*., 1990; Apte *et al*., 1994; Greene *et al*., 1996). Each is a protein of around 190 residues containing six disulfide bonds (Williamson *et al*., 1990). TIMP-1, -2, and -3 can inhibit all members of the MMP family but show differences in their specificity for membrane type-1 MMP (Will *et al*., 1996) and in their ability to form stable complexes with the pro form of the enzymes.

Both the MMPs and the TIMPs consist of distinct functional domains. The MMPs consist of a pro peptide which is required for latency, a catalytic domain containing the active site zinc ion, and, except for MMP-7, a C-terminal domain that has structural homology with hemopexin (Matrisian, 1992; Birkedal-Hansen, 1995). The catalytic domain (N-MMP, 19.4 kDa) can be expressed independently of the other domains to give a folded protein with full enzymatic activity, and the ability to form stable inhibitory complexes with TIMPs (Marcy *et al*., 1991; Nguyen *et al*., 1994). The TIMPs appear to consist of two domains, although only one, the N-terminal domain (N-TIMP), has been expressed as an independent unit (Murphy *et al*., 1991). This domain, encompassing about 65% of the molecule and three of the six disulfide bonds, retains TIMP activity and is able to form stable inhibitory complexes with both active full-length MMPs and their separate catalytic domains (Willenbrock *et al*., 1993; Nguyen *et al*., 1994). High-resolution crystal and NMR structures are now available for several MMP catalytic domains, including human MMP-1 (Borkakoti *et al*., 1994; Lovejoy *et al*., 1994; Spurlino *et al*., 1994), human MMP-3 (Becker *et al*., 1995; Van Doren *et al*., 1995; Gooley *et al*., 1996), and human MMP-8 (Bode *et al*., 1994; Stams *et al*., 1994), and in 1994, we published the first three-dimensional structure for human N-TIMP-2 obtained with 2D and 3D ^{1}H NMR (Williamson *et al*., 1994).

The region of N-TIMP responsible for the interaction with the MMPs has not yet been identified. Several studies have investigated TIMP binding using a wide variety of techniques, for example site-directed mutagenesis (O'Shea *et al*., 1992; Murphy *et al*., 1997), chemical modification (Williamson *et al*., 1993), and MMP inhibition by TIMP peptide fragments (Hanglow *et al*., 1994; Bodden *et al*., 1994), but no clear picture of the binding site has emerged. Kinetic data on the interaction between TIMPs and MMPs suggest multisite binding (Willenbrock *et al*., 1993; Murphy & Willenbrock, 1995), and this may hamper the success of those approaches where only one or a few residues are altered or replaced at any one time. Our work, presented here, maps the interaction site on N-TIMP-2 by analyzing the change in the NMR chemical shift of the ^{1}H and ^{15}N nuclei

† This work was funded by the Arthritis and Rheumatism Council (U.K.) and Medical Research Council (U.K.).

* To whom correspondence should be addressed: Dr. R. A. Williamson, Department of Biosciences, University of Kent, Canterbury, Kent CT2 7NJ, U.K. Telephone: 01227 764000, ext 7012 or 7598. Fax: 01227 763912. E-mail: r.a.williamson@ukc.ac.uk.

‡ University of Kent.

§ MRC Biomedical NMR Centre, National Institute for Medical Research.

|| Division of Molecular Structure, National Institute for Medical Research.

⊗ Abstract published in *Advance ACS Abstracts,* September 15, 1997.

[1] Abbreviations: 2D, two-dimensional; 3D, three-dimensional; MMP, matrix metalloproteinase; N-MMP, N-terminal domain of MMP; TIMP, tissue inhibitor of metalloproteinase; N-TIMP, N-terminal domain of TIMP.

S0006-2960(97)01209-9 CCC: $14.00 © 1997 American Chemical Society

of backbone amide groups of N-TIMP-2 on binding to the catalytic domain of human stromelysin-1 (N-MMP-3). The chemical shift of a particular nucleus is dependent on its environment; hence, this technique identifies those residues which undergo an environment change on binding, namely those residues at the interaction site or those which undergo a conformational change induced by complex formation. A full analysis by this method would involve complete sequence-specific assignment of the amide ^{1}H and ^{15}N chemical shifts for both free and bound N-TIMP-2 to determine the true chemical shift changes on complex formation. However, once the sequence-specific assignments have been made for the free protein, a simple procedure of measuring chemical shift changes to the nearest peak in the complex (hence, determining a lower limit to the actual shift) provides a convenient method of mapping the extent and overall properties of the interaction site (Farmer *et al*., 1996).

MATERIALS AND METHODS

^{15}N/^{13}C-Labeled N-TIMP-2. Human N-TIMP-2 was expressed in *Escherichia coli* and refolded from insoluble inclusion bodies as described by Williamson *et al*. (1996). To produce uniformly ^{15}N/^{13}C-labeled protein, the transformed *E. coli* cells were grown from a single colony in minimal media containing 0.6 g/L [^{15}N]ammonium sulfate (99.5% ^{15}N; Isotec Inc., Miamisburg, OH) as the sole nitrogen source and 2.0 g/L [^{13}C]-D-glucose (97% ^{13}C; Isotec Inc.) as the sole carbon source. The cultures were induced at an A_{600nm} of 0.85 with 0.45 mM IPTG and the cells harvested after a further 3 h of incubation at 37 °C. Yields of 8 mg of purified protein per liter of culture were routinely obtained. The degree of isotope replacement for ^{15}N/^{13}C-labeled N-TIMP-2 was found to be greater than 95% as measured by electrospray mass spectrometry.

N-MMP-3. DNA (pET19) containing the coding region for the pro and catalytic domains of human MMP-3 (stromelysin-1) was kindly provided by A. Marcy (Merck). Expression and purification of the pro protein were carried out as previously described (Marcy *et al*., 1991). Pro-N-MMP-3 was activated at a concentration of 2 mg/mL with 2 mM APMA at 35 °C for 16 h and residual APMA removed by dialysis against 20 mM Tris-HCl, 5 mM $CaCl_2$, and 0.02% w/v NaN_3 at pH 8.0 and 4 °C.

N-TIMP-2/N-MMP-3 Complex. The complex was prepared by incubating ^{15}N/^{13}C-labeled N-TIMP-2 at 1 mg/mL with an equimolar amount of N-MMP-3 in 20 mM Tris-HCl, 5 mM $CaCl_2$, and 0.02% w/v NaN_3 at pH 8.0 for 16 h at 4 °C. Ten milliliter aliquots of this mixture were separated on a Sephacryl S100 (Pharmacia) gel filtration column (2.6 × 36 cm) equilibrated in 5 mM deuterated imidazole/sodium hydroxide, 100 mM NaCl, 5 mM $CaCl_2$, and 0.02% w/v NaN_3 at pH 6.4. The N-TIMP-2/N-MMP-3 complex eluted at 105 mL, free N-TIMP-2 at 125 mL, and free N-MMP-3 at 130 mL. An estimation of the protein concentration on SDS−PAGE showed that over 90% of the N-TIMP-2 formed a stable complex with N-MMP-3. The fractions containing the complex were pooled, concentrated by ultrafiltration, and then freeze-dried.

NMR Measurements. The NMR experiments were carried out on Varian Unity spectrometers operating at 500 and 600 MHz, with all the data collected in the phase-sensitive mode using the method of States *et al*. (1982). ^{15}N/^{1}H and ^{13}C/^{1}H HMQC (Bax *et al*., 1983), HCCH-TOCSY (Bax *et al*., 1990), and CBCANH (Grzesiek & Bax, 1992) spectra were recorded at 35 °C from 0.6 mL samples of 1.4 mM uniformly ^{15}N/^{13}C-labeled N-TIMP-2 dissolved in 25 mM sodium phosphate buffer and 100 mM potassium chloride at pH 6.7. In addition, ^{15}N/^{1}H HSQC (Bodenhausen & Rubens, 1980) and ^{13}C/^{1}H HMQC spectra were acquired at 35 °C from a 0.4 mM solution of the tight complex formed between ^{15}N/^{13}C-labeled N-TIMP-2 and N-MMP-3 in 5 mM deuterated imidazole/sodium hydroxide and 100 mM sodium chloride at pH 6.7. The samples were prepared in either 100% D_2O or 90% H_2O/10% D_2O as was appropriate.

In the HCCH-TOCSY experiments, isotropic mixing of ^{13}C for periods of 13 or 20 ms was carried out with a DIPSI-3 pulse sequence at a radio frequency field strength of 7.5−8.3 kHz (Shaka *et al*., 1988). The decoupling of ^{15}N and ^{13}C from ^{1}H during the acquisition time was achieved by using the GARP1 sequence with fields of 1.1 and 3.1−3.3 kHz, respectively (Shaka *et al*., 1985). For the CBCANH experiment, ^{1}H decoupling was performed with a DIPSI-2 scheme at a field strength of 5.7 kHz (Shaka *et al*., 1988). The 3D experiments required the use of off-resonance selective ^{13}C pulses, such as the carbonyl and aromatic inversion pulses included in the HCCH-TOCSY sequence. To avoid explicitly changing the frequency of the ^{13}C carrier, the so-called phase-modulation approach was used to obtain all these frequency-shifted pulses (Boyd & Soffe, 1989). The amplitude profile of the selective carbonyl and aromatic pulses consisted of the central lobe of a $\sin(x)/x$ function, and the pulses were 195−348 μs in duration. In the HSQC, HCCH-TOCSY, and CBCANH experiments, a combination of phase cycling and pulsed-field gradient pulses was used to suppress artifacts. The gradient pulses were incorporated into the sequences at positions that resulted in no significant reduction in the intensity of desired signals (Bax & Pochapsky, 1992). For the 2D ^{15}N/^{1}H HMQC experiments, water suppression was achieved by using selective presaturation at the water frequency; however, all the other spectra recorded from samples in 90% H_2O/10% D_2O employed the pulsed-field gradient-based WATERGATE method (Sklenar *et al*., 1993).

The 2D spectra were collected over a period of 14−16 h with acquisition times of 40−66 ms in F_1 and 128−146 ms in F_2. The 3D spectra were acquired over 64−88 h with acquisition times in the indirectly detected dimensions (F_1 or F_2) of 15.3 ms for ^{15}N, 6.3−9.7 ms for ^{13}C, and 16−18.6 ms for ^{1}H, as was appropriate, and in the real time domain (F_3) of 51−64 ms. In the HCCH-TOCSY experiments, folding of ^{13}C resonances was used to obtain increased resolution.

The 2D data were processed on SUN workstations using the Varian VNMR software package. The original data were typically zero-filled twice in F_1 and once in F_2 prior to Fourier transformation, and mild resolution enhancement was achieved by applying a π/3-shifted sine-squared apodization function in both dimensions. The 3D spectra were transformed using software written at the MRC Biomedical NMR Centre (C. J. Bauer, unpublished work) and installed on a SUN SPARCstation 10. To improve the resolution in the final spectra, the number of data points in F_1 and F_2 was initially extended by a factor of 1.5−2 using linear prediction (Press *et al*., 1988), and then the time domain matrixes were zero-filled at least once in all dimensions. Mild resolution

enhancement was obtained by applying a $\pi/2.5$-shifted sine-squared apodization function in all dimensions. All the spectra were analyzed on-screen using the program XEASY (Bartels *et al.*, 1995).

RESULTS AND DISCUSSION

Sequence-Specific ^{15}N, ^{13}C, and ^{1}H Resonance Assignments for Free N-TIMP-2. Previously, we have reported essentially complete sequence-specific ^{1}H resonance assignments for N-TIMP-2 (Williamson *et al.*, 1994). This work has now been extended to obtain ^{15}N and ^{13}C resonance assignments using a combination of 3D HCCH-TOCSY and CBCANH experiments on uniformly $^{15}N/^{13}C$-labeled protein. In the CBCANH spectra, both intraresidue and sequential through-bond correlations from Cα and (for non-glycine residues) Cβ atoms to amide nitrogen/proton pairs were seen for all residues in the sequence stretches C3−A66 and C72−E127, with the exception of six breaks corresponding to proline residues at positions 5, 8, 39, 56, 67, and 106. The chemical shifts obtained for backbone amide and methyl groups from the CBCANH and HCCH-TOCSY data (see the Supporting Information) were entirely consistent with those obtained from earlier analyses of 2D ^{1}H spectra (Williamson *et al.*, 1994).

Through-bond connectivities (intraresidue or sequential) could not be identified in the CBCANH spectrum for residues C1−S2 or S68−V71, which are linked together in the protein by the C1−C72 disulfide bond. The reason for their absence from the CBCANH data is unclear, but consistent with the fact that no backbone amide ^{1}H assignments could be made for this region in earlier 2D ^{1}H studies (Williamson *et al.*, 1994). In contrast, ^{1}H and ^{13}C assignments have been obtained for the side chains and backbone signals for all of these residues (Williamson *et al.*, 1994; unpublished data). The inability to detect the backbone amide ^{1}H and ^{15}N resonances in this region almost certainly arises because these signals are significantly broadened compared to signals from other backbone groups in the protein. This localized signal broadening could occur if the region exists in several conformational states in intermediate exchange on the NMR chemical shift time scale. However, the side chain resonances are unaffected so such a mixture of conformations would need to influence the shielding of backbone NH nuclei more than the side chain nuclei. Another possibility is that the amide line broadening occurs via rapid exchange with water catalyzed by the local environment of the region. Analysis of the N-TIMP-2 structure reveals that the S68−C72−C1−C3 region forms a "ridge" of extended polypeptide that is highly exposed on the surface of the protein.

Chemical Shift Changes Seen on Complex Formation with N-MMP-3. $^{15}N/^{1}H$ HMQC or HSQC spectra were collected for both free $^{15}N/^{13}C$-labeled N-TIMP-2 and the purified complex of $^{15}N/^{13}C$-labeled N-TIMP-2 with nonlabeled N-MMP-3 (Figure 1). The N-TIMP-2/N-MMP-3 complex proved to be sufficiently stable to allow purification as a single molecule by gel-filtration chromatography, and there was no evidence of signals from free N-TIMP-2 in the spectrum of the complex. The line widths for N-TIMP-2 were significantly broader in the spectrum of the complex, as expected for an effective increase in the molecular mass of N-TIMP-2 from 14.1 to 33.5 kDa (Figure 1). Nevertheless, the resolution of the spectrum for the complex is

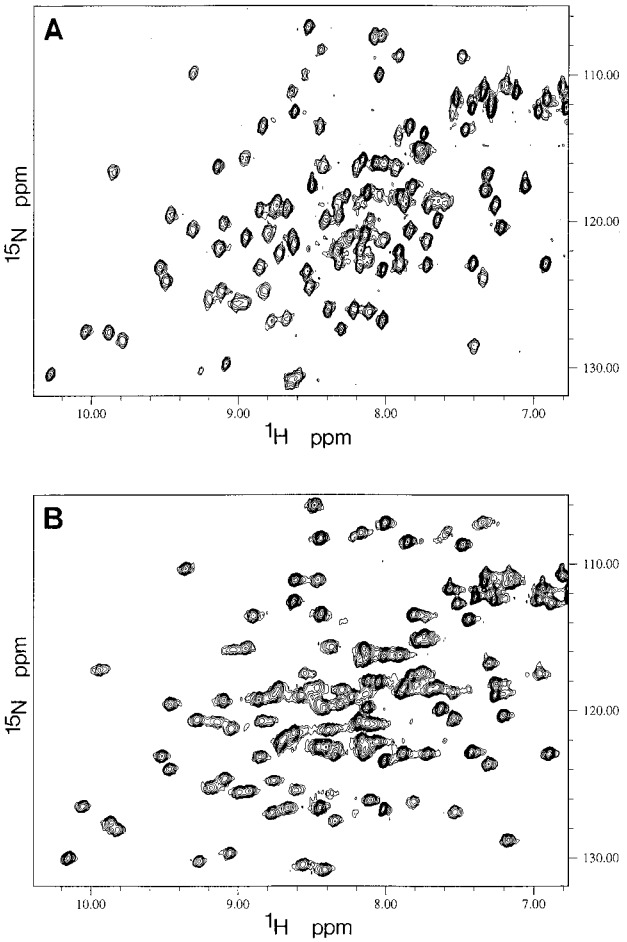

FIGURE 1: $^{15}N/^{1}H$ HMQC spectrum of free $^{15}N/^{13}C$-labeled N-TIMP-2 (A) and $^{15}N/^{1}H$ HSQC spectrum of the complex of $^{15}N/^{13}C$-labeled N-TIMP-2 with unlabeled N-MMP-3 (B). The chemical shifts of 60−70% of the backbone amide cross-peaks were unaffected by N-MMP-3 binding.

sufficiently high to allow the majority (>85%) of the $^{15}N/^{1}H$ amide cross-peaks of N-TIMP-2 to be resolved. Cross-peaks from backbone amide groups in the $^{15}N/^{1}H$ HMQC spectrum of free N-TIMP-2 were easily assigned by reference to the ^{1}H and ^{15}N resonance frequencies determined from the CBCANH experiment.

An overlay of the two spectra for free and N-MMP-3-bound N-TIMP-2 (Figure 1) revealed that about 60−70% of the $^{15}N/^{1}H$ backbone amide cross-peaks for free N-TIMP-2 were apparently unaffected by complex formation (that is, neither the ^{1}H nor ^{15}N chemical shifts appeared to be significantly altered). A study of the overlaid spectra allowed many of the unchanged cross-peaks to be tentatively assigned in the complex on the basis of a simple "pattern matching" approach. For the signals which had moved, the chemical shift difference to the nearest cross-peak was measured since this places a lower limit on the chemical shift changes experienced by the NH nuclei. Farmer *et al.* (1996) used a similar approach to map the binding site of $NADP^{+}$ on the MurB enzyme. The nearest signal was judged by considering both the ^{1}H and ^{15}N chemical shift changes. The shift used for ^{15}N was scaled for the difference in the spectral width of the backbone ^{15}N resonances relative to the ^{1}H signals to try to give a roughly equal weighting for each (^{15}N range, 130.8 − 108.8 ppm = 22.0 ppm; ^{1}H range, 10.04 − 6.92 ppm = 3.12 ppm; correction factor of $^{1}/_{7}$). With the calculation of the sum of the magnitudes of the changes in

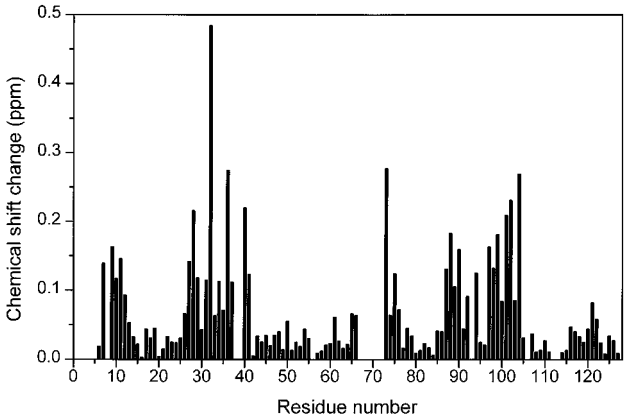

FIGURE 2: Chemical shift changes for each backbone amide group of N-TIMP-2 on complex formation with N-MMP-3. The chemical shift change was measured from the $^{15}N/^{1}H$ cross-peak of the backbone amide group of each residue in the spectrum of free N-TIMP-2 to the nearest $^{15}N/^{1}H$ cross-peak in the spectrum of the N-TIMP-2/N-MMP-3 complex using the relationship $\Delta^1H + \Delta^{15}N/7$ ($\Delta^1H + \Delta^{15}N/5$ for glycine residues).

^{1}H and corrected ^{15}N chemical shifts (Δ^1H and $\Delta^{15}N/7$, respectively), the nearest peak was determined to be that with the lowest score. Glycine amide groups form a distinct subset with a chemical shift spread different from those of the rest of the amino acid residue types (Wishart *et al*., 1991) and hence were treated separately (^{15}N range, 113.5 − 106.8 ppm = 6.7 ppm; ^{1}H range, 9.31 − 7.91 ppm = 1.40 ppm; correction factor of $^{1}/_{5}$).

Regions of N-TIMP-2 Perturbed by Binding to N-MMP-3. The backbone amide chemical shift change for each residue in N-TIMP-2 on formation of the N-MMP-3 complex is shown in Figure 2. Residues C1, S2, and S68−V71 are missing from the analysis as their backbone amide resonances could not be identified in the CBCANH experiment. Residues C3, S4, C72, D93, T112, and T113 were not included in the analysis because these residues showed only very weak $^{15}N/^{1}H$ correlations in the HMQC spectrum of free N-TIMP-2, and so with the broader line widths in the spectrum of the complex, we could not assume that these signals would remain detectable.

Residues with large chemical shift changes of their backbone amide group were found to cluster in several regions of the N-TIMP-2 sequence, in particular, H7−A11, K27−K41, G73−S75, A87−A90, and H97−I104 (Figure 2). To simplify the analysis, the changes in the backbone amide chemical shift were divided into four categories and displayed on a loop diagram of the N-TIMP-2 primary structure (Figure 3). The classification is arbitrary but was based on an analysis of Figure 2 and a plot of the amide chemical shift changes in ascending order of size (data not shown) which suggested four groups (0−0.05 ppm classified as "nonshifted" amide groups, 0.05−0.10 ppm "slightly shifted" amide groups, 0.10−0.20 ppm "shifted" amide groups, and >0.20 ppm "highly shifted" amide groups). The regions of N-TIMP-2 with shifted and highly shifted backbone amide chemical shift changes on binding to N-MMP-3 map onto the structure of the protein as follows: (1) H7 and the residues of helix 1 up to A11, (2) the C-terminal half of strand A, the AB β-turn, and the first four residues of strand B, (3) G73−S75 in the long loop between strands C and D, (4) the C-terminal half of strand D and G94 in the tight turn between strands D and E, and (5) the C-terminal half of strand E and the loop between strands E and F containing the C3−C101 disulfide bond. The four categories of chemical shift changes are shown on a ribbon diagram of the N-TIMP-2 structure in Figure 4A. More than half the structure (66 residues) had no significant changes in amide chemical shifts. The largest chemical shift changes occurred in the long stretch from E26 to K41 and in the loop between strands E and F.

MMP Binding Site on N-TIMP-2. The residues with significantly shifted amide resonances form a broad site covering most of one face of the N-TIMP-2 molecule (Figure 4B). The structural proximity of the most strongly shifted residues suggests that the chemical shift changes arise from these residues being directly involved in complex formation (or from local conformational changes) and hence defining a binding site. The site stretches across the top lip and side of the core β-barrel of N-TIMP-2 centered approximately on strand E. The left-hand side of the site (as orientated in Figure 4A,B) is defined by strands A and B and the AB β-turn, while the right-hand side extends to helix 1. Running across the center of the site and forming a surface ridge is the extended stretch C1−S4 and S68−C72 connected by the C1−C72 disulfide bond. There are no backbone amide chemical shift data for this region, but its prominent position within the site clearly suggests a role in MMP binding. Rotation of the model in Figure 4B through approximately 180° generates the view shown in Figure 4C. The lack of shifted backbone amide groups on this face of the protein clearly suggests that the chemical shift changes induced by complex formation are specific for the N-MMP-3 binding site, and that the inhibitor does not undergo a large overall conformational change on binding.

The identification of the N-MMP-3 binding site was further supported by analysis of data from similar heteronuclear NMR experiments measuring cross-peak shifts for methyl groups in $^{13}C/^{1}H$ HMQC spectra of free and N-MMP-3-bound $^{15}N/^{13}C$-labeled N-TIMP-2 (Figure 5). The residues with highly shifted methyl groups were A11, I35, I40, A66, V71, and L100, and all of these form part of the binding site shown in Figures 3 and 4. Interestingly, four methyl cross-peaks showed considerable chemical shift changes on complex formation (>0.5 ppm for Δ^1H alone) but remained unassigned using the "nearest peak" approach described here due to their large shifts from a relatively crowded region of the spectrum.

A feature of the N-MMP-3 binding site appears to be its flexibility. The region D30−K41 (the end of strands A and B and the AB β-turn) showed no detectable NOEs to other parts of the molecule in earlier work (Williamson *et al*., 1994), although many NOEs were identified between the two strands. This finding suggested that this region of N-TIMP-2 is flexible, and thus able to move independently through a relatively large conformational space, with the β-bulge at S31 and G32 possibly acting as a hinge. This region contains some of the largest changes in amide chemical shifts and is therefore intimately involved with N-MMP-3 binding, or a resultant local conformational change. This "arm" may adopt a more stable conformation on binding of the MMP, either by interacting directly with the enzyme or possibly by being forced to one side as the enzyme binds to a site on the core of the N-TIMP-2 β-barrel. The other flexible region involved with N-MMP-3 binding is the extended sequence comprising C1−S2 and S68−V71 linked by the C1−C72 disulfide

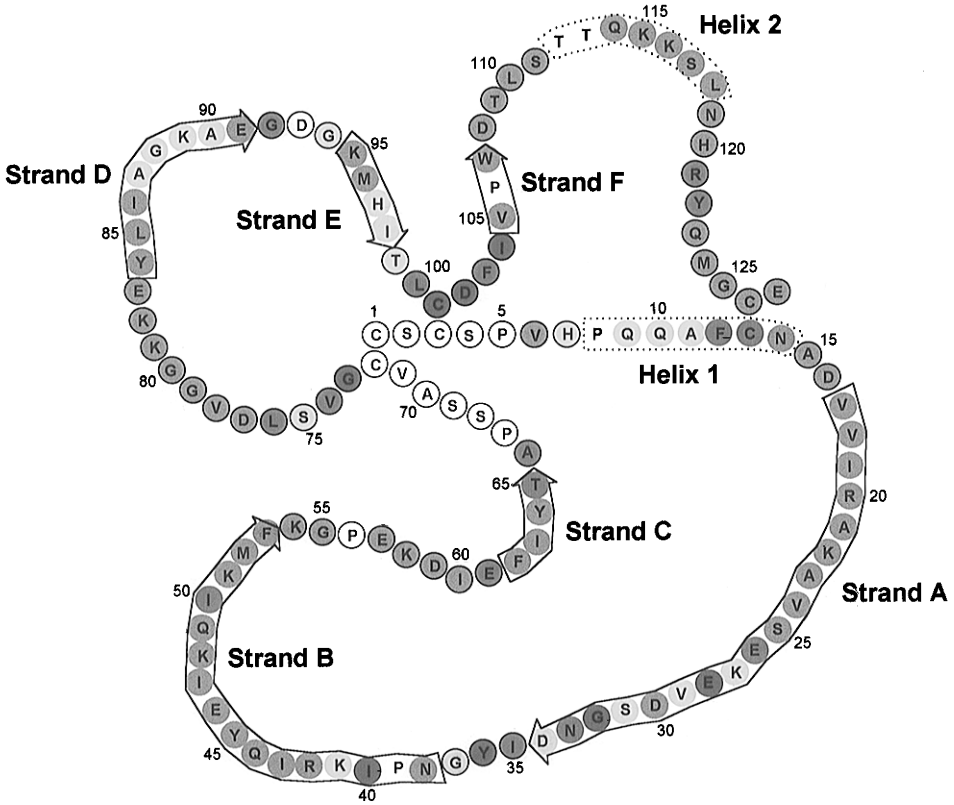

FIGURE 3: Loop diagram of the primary and secondary structure of N-TIMP-2 showing the chemical shift changes for the backbone amide groups of N-TIMP-2 on complex formation with N-MMP-3. The chemical shift changes ($\Delta^1H + \Delta^{15}N/7$ or $\Delta^1H + \Delta^{15}N/5$ for glycine residues) were classified into four groups indicated by different colors: blue, 0.00−0.05 ppm; green, 0.05−0.10 ppm; yellow, 0.10−0.20 ppm; and red, >0.20 ppm. Residues for which no chemical shift information was obtained are shown in white.

bond. This stretch showed no detectable NH signals in the CBCANH spectrum of free N-TIMP-2, which could be due to exchange between several conformational states as discussed above.

Relationship with Other Surface Sites. In our previous work (Williamson *et al*., 1994), two surface sites on N-TIMP-2 were identified with potential functional importance. The first, the OB binding site, was identified by structural homology of N-TIMP-2 with proteins of the OB (oligonucleotide/oligosaccharide binding) fold family, where a common region for ligand binding is seen (Murzin, 1993). This region is broad and does not define structurally homologous residues important for binding; however, all ligand binding sites identified for the OB-fold protein family fall on one face of the molecule made up of the ends of strands A and B and the AB turn, the ends of strands D and E and the DE turn, and strand C, and part of the CD loop. For some OB-fold proteins, the N terminus also extends into this site. Interestingly, the MMP binding site identified in this work overlaps considerably with the OB binding site. The regions in common include the ends of strands A and B and the AB turn, the C-terminal portion of strand D, and the N-terminal region of the molecule. Most of the loop between strands E and F also falls in the region of the OB binding site in N-TIMP-2. This loop is not present in other members of the OB-fold protein family, although a smaller β-bulge is often found in a homologous position (Murzin, 1993).

The second potentially important surface site on N-TIMP-2 was identified by amino acid sequence conservation across the TIMP family. This site, which is quite hydrophobic in nature, consisted of residues H7, L85, F103, W107, Q114, L118, and Y122 (Williamson *et al*., 1994). Residues homologous to H7 and W107 were mutated in TIMP-1 and found to affect inhibition and binding to MMP-7 (O'Shea *et al*., 1992). Apart from it being a potential MMP binding site, we also proposed that this region was a good candidate for the site of interaction of the C-terminal domain of TIMP-2 as it is near the C terminus of the N-TIMP-2 molecule. This proposal has gained some support from recent kinetic studies (Murphy *et al*., 1997) which have shown that mutants of H7 and Q9 in TIMP-1 bind to MMP-2 and MMP-3 with rates (k_{on}) similar to that of the truncated molecule (N-TIMP-1). One possible interpretation is that the effect of the mutation is to abolish the binding contribution provided by the C-terminal domain of TIMP-1, possibly by perturbing the orientation of the two domains so that they can no longer act cooperatively. Our data are consistent with this theory. The conserved surface patch is on the far right-hand side of N-TIMP-2 as shown in Figure 4B, and although the site overlaps at H7, F103, and Y122, two of these residues experience only slight changes in amide chemical shift and all fall on the edge of the proposed MMP binding site.

Sequence Conservation and Site-Directed Mutagenesis Data. An interesting feature of the MMP binding site is the fact that some of its regions are poorly conserved between different TIMP sequences, in particular, the ends of strands A and B and the AB turn. This region is absent from TIMP-1 (a deletion of seven residues), with the proposed structural consequence being that the AB turn occurs earlier in the sequence starting at the N-glycosylated Asn30 (Williamson *et al*., 1994). This structural difference suggests that this region is not responsible for direct inhibition of the MMPs but nevertheless interacts, and may be pushed aside,

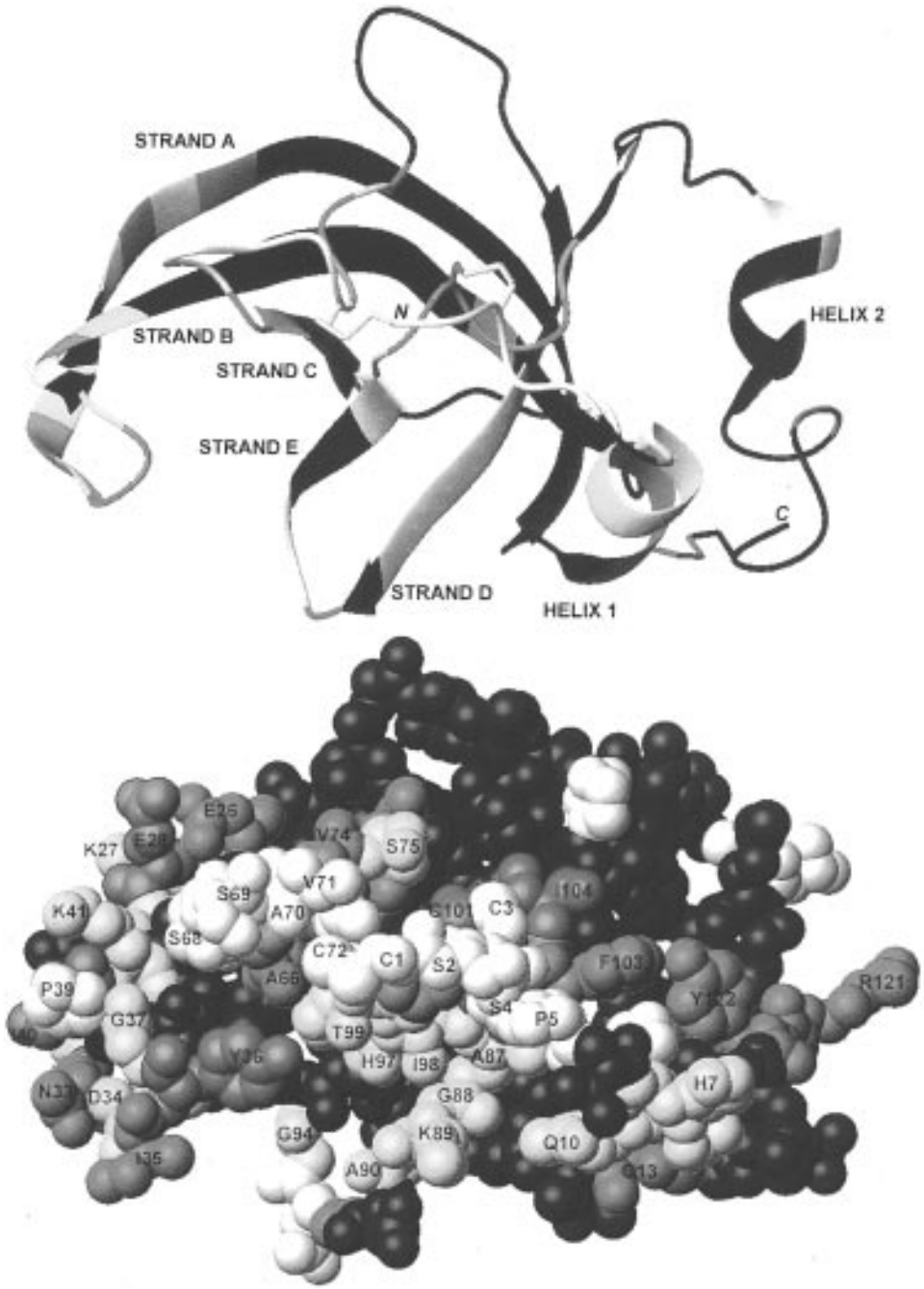

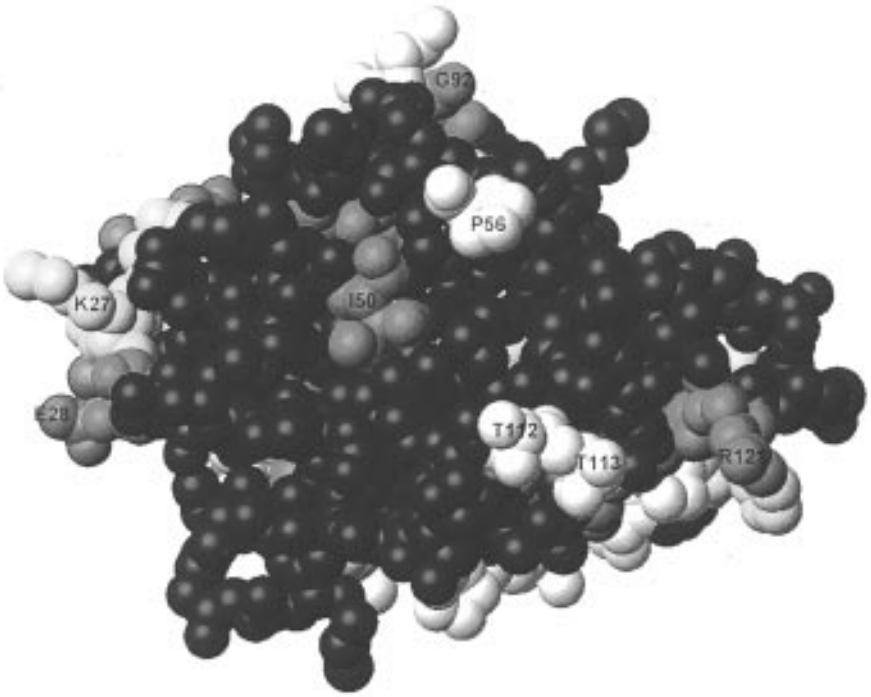

FIGURE 4: Three different views of N-TIMP-2 showing the position of the proposed MMP binding site. Residues are colored according to the chemical shift change of their backbone amide group as defined in Figure 3: (A, left) a ribbon diagram of the α-carbon backbone of N-TIMP-2 orientated with the MMP binding site at the front of the molecule, (B, bottom) a space-filled model of N-TIMP-2 (without hydrogen atoms) in the same orientation as panel A, and (C, top right) a space-filled model of the "backside" of N-TIMP-2 (generated from view B by a rotation of about 180° along the *x*-axis) showing that there are essentially no residues with shifted backbone amide signals on this face of the molecule. This figure was produced using MOLMOL (Koradi *et al.*, 1996).

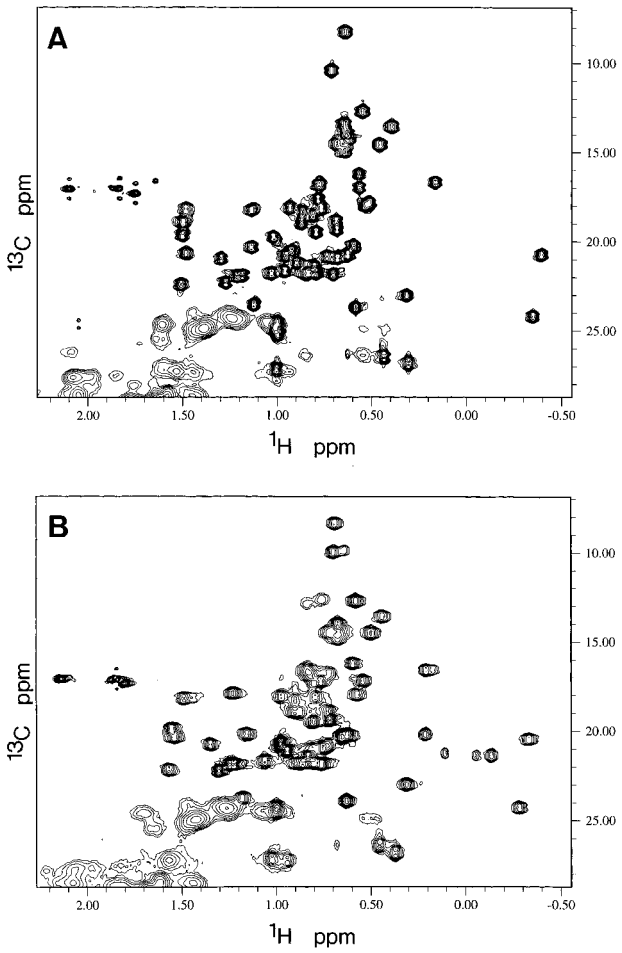

FIGURE 5: Methyl region from ^{13}C/^{1}H HSQC spectra of free ^{15}N/^{13}C-labeled N-TIMP-2 (A) and the complex with unlabeled N-MMP-3 (B). Four peaks show considerable chemical shift changes on complex formation (>0.5 ppm for Δ^{1}H alone) and are seen in the bottom right-hand side of spectrum B.

by the bound enzyme.

The most highly conserved regions of the MMP binding site are H7 and helix 1, and the region around the C1−C72 and C3−C101 disulfide bonds (C1−C3, V71−V74, and C101−I104). The functional importance of H7 and helix 1 was probed by site-directed mutagenesis (O'Shea *et al*., 1992), and apart from mutations at H7 and Q9 (discussed earlier), no other residues in this region appeared to directly influence the kinetics of TIMP-1 binding to MMP-2. The region around the C1−C72 and C3−C101 disulfide bonds contains fewer identical residues and has only recently been the target of site-directed mutagenesis studies. However, this region appears to be important for TIMP-1 activity as when residue T2 (homologous to S2 in TIMP-2) was mutated to Ala a significant increase in the K_i of TIMP-1 binding to N-MMP-3 (more than 100-fold) was measured (Nagase *et al*., 1997). Furthermore, proteolytic cleavage of the V69−C70 peptide bond in TIMP-1 by human neutrophil elastase has been shown to result in TIMP-1 inactivation, while the cleavage at this site was protected by complex formation with MMP-3 (Nagase *et al*., 1997). These findings are entirely consistent with the MMP binding site mapped in this NMR study. The region around disulfides C1−C72 and C3−C101 falls in the center of the proposed MMP binding site and contains four of the eight most highly shifted backbone amide groups (G73, C101, D102, and I104).

The remainder of the MMP binding site is relatively poorly conserved and thus remains largely unexplored by site-directed mutagenesis, except for H97. The homologous residue in TIMP-1 (H95) was originally identified by chemical modification as potentially important for MMP inhibition (Williamson *et al*., 1993), but subsequent mutagenesis studies of this residue have reported contradictory results. O'Shea *et al*. (1992) found that mutation of H95 to Ala or Gln in TIMP-1 had no effect on the rate of MMP-7 binding or MMP-3 inhibition, although Walther *et al*. (1997) have reported that mutation of H95 to Arg affects TIMP-1 activity *in vivo*.

The NMR work presented here provides the first direct evidence for the location, extent, and composition of the MMP binding site on the N-terminal domain of TIMP-2. The role and importance of particular residues can now be explored further by site-directed mutagenesis studies. With the recent publication of heteronuclear assignments and NMR structures for N-MMP-3 (Gooley *et al*., 1993, 1996; Van Doren *et al*., 1993, 1995), it will be possible to map the N-TIMP-2 binding site on the catalytic domain of the enzyme with a similar chemical shift-based approach. This work provides a valuable method of understanding the mechanism of inhibition of the MMPs by their natural inhibitor TIMP.

ACKNOWLEDGMENT

The authors thank Prof. Gillian Murphy and Dr. Andrew Docherty for valuable discussion and advice. The NMR spectra were recorded using facilities at the Medical Research Council Biomedical NMR Centre, NIMR, Mill Hill.

SUPPORTING INFORMATION AVAILABLE

^{15}N, ^{13}C, and ^{1}H assignments for backbone amide and methyl groups of N-TIMP-2 (3 pages). Ordering information is given on any current masthead page.

REFERENCES

Apte, S. S., Mattei, M.-G., & Olsen, B. R. (1994) *Genomics 19*, 86−90.

Bartels, C., Xia, T., Billeter, M., Güntert, P., & Wüthrich, K. (1995) *J. Biomol. NMR 5*, 1−10.

Bax, A., & Pochapsky, S. S. (1992) *J. Magn. Reson. 99*, 638−643.

Bax, A., Griffey, R. H., & Hawkins, B. L. (1983) *J. Am. Chem. Soc. 105*, 7188−7190.

Bax, A., Clore, G. M., & Gronenborn, A. M. (1990) *J. Magn. Reson. 88*, 425−431.

Becker, J. W., Marcy, A. I., Rokosz, L. L., Axel, M. G., Burbaum, J. J., Fitzgerald, P. M. D., Cameron, P. M., Esser, C. K., Hagmann, W. K., Hermes, J. D., & Springer, J. P. (1995) *Protein Sci. 4*, 1966−1976.

Birkedal-Hansen, H. (1995) *Curr. Opin. Cell Biol. 7*, 728−735.

Bodden, M. K., Harber, G. J., Birkedal-Hansen, B., Windsor, Caterina, N. C., Engler, J. A., & Birkedal-Hansen, H. (1994) *J. Biol. Chem. 269*, 18943−18952.

Bode, W., Reinemer, P., Huber, R., Kleine, T., Schniere, S., & Tschesche, H. (1994) *EMBO J. 13*, 1263−1269.

Bodenhausen, G., & Ruben, D. J. (1980) *Chem. Phys. Lett. 69*, 185−189.

Boone, T. C., Johnson, M. J., DeClerck, Y. A., & Langley, K. E. (1990) *Proc. Natl. Acad. Sci. U.S.A. 87*, 2800−2804.

Borkakoti, N., Winkler, F. K., Williams, D. H., D'Arcy, A., Broadhurst, M. J., Brown, P. A., Johnson, W. H., & Murry, E. J. (1994) *Nat. Struct. Biol. 1*, 106−110.

Boyd, J., & Soffe, N. (1989) *J. Magn. Reson. 85*, 406−413.

Docherty, A. J. P., Lyons, A., Smith, B. J., Wright, E. M., Stephens, P. E., Harris, T. J. R., Murphy, G., & Reynolds, J. J. (1985) *Nature 318*, 66−69.

Docherty, A. J. P., O'Connell, J., Crabbe, T., Angal, S., & Murphy, G. (1992) *Trends Biotechnol. 10*, 200−207.

Farmer, B. T., Constantine, K. L., Goldfarb, V., Friedrichs, M. S., Wittekind, M., Yanchunas, J., Robertson, J. G., & Mueller, L. (1996) *Nat. Struct. Biol. 3*, 995−997.

Gooley, P. R., Johnson, B. A., Marcy, A. I., Cuca, G. C., Salowe, S. P., Hagmann, W. K., Esser, C. K., & Springer, J. P. (1993) *Biochemistry 32*, 13098−13108.

Gooley, P. R., O'Connell, J. F., Marcy, A. I., Cuca, G. C., Axel, M. G., Caldwell, C. G., Hagmann, W. K., & Becker, J. W. (1996) *J. Biomol. NMR 7*, 8−28.

Greene, K., Wang, M., Liu, Y., Raymond, L. A., Rosen, C., & Shi Y. E. (1996) *J. Biol. Chem. 271*, 30275−30380.

Grzesiek, S., & Bax, A. (1992) *J. Magn. Reson. 99*, 201−207.

Hanglow, A. C., Lugo, A., Walsky, R., Visnick, M., Coffey, J. W., & Fotouhi (1994) *Biochem. Biophys. Res. Commun. 205*, 1156−1163.

Koradi, R., Billeter, M., & Wuthrich, K. (1996) *J. Mol. Graphics 14*, 51−55.

Lovejoy, B., Cleasby, A., Hassell, A., Longley, K., Luther, M. A., Weigl, D., McGeehan, G., McElroy, A. B., Drewry, D., Lambert, M. H., & Jordan, S. R. (1994) *Science 263*, 375−377.

Marcy, A. I., Eiberger, L. L., Harrison, R., Chan, H. K., Hutchinson, N. I., Hagmann, W. K., Cameron, P. M., Boulton, D. A., & Hermes, J. D. (1991) *Biochemistry 30*, 6476−6483.

Matrisian, L. M. (1992) *BioEssays 14*, 455−463.

Murphy, G., & Willenbrock, F. (1995) *Methods Enzymol. 248*, 496−510.

Murphy, G., Houbrechts, A., Cockett, M. I., Williamson, R. A., O'Shea, M., & Docherty, A. J. P. (1991) *Biochemistry 30*, 8097−8102.

Murphy, G., Butler, G., Knauper, V., O'Shea, M., Williamson, R., Docherty, A., Apte, S., & Willenbrock, F. (1997) in *Inhibitors of Metalloproteinases in Development and Disease* (Hawkes, S. P., Edwards, D. R., & Khokha, D., Eds.) Harwood Academic Publishing, Lausanne, Switzerland.

Murzin, A. G. (1993) *EMBO J. 12*, 861−867.

Nagase, H., Das, S. K., Dey, S. K., Fowlkes, J. L., Huang, W., & Brew, K. (1997) in *Inhibitors of Metalloproteinases in Development and Disease* (Hawkes, S. P., Edwards, D. R., & Khokha, R., Eds.) Harwood Academic Publishing, Lausanne, Switzerland.

Nguyen, Q., Willenbrock, F., Cockett, M. I., O'Shea, M., Docherty, A. J. P., & Murphy, G. (1994) *Biochemistry 33*, 2089−2095.

O'Shea, M., Willenbrock, F. W., Williamson, R. A., Cockett, M. I., Freedman, R. B., Reynolds, J. J., Docherty, A. J. P., & Murphy, G. (1992) *Biochemistry 31*, 10146−10152.

Press, W. H., Flannery, B. P., Teukolsky, S. A., & Vetterling, W. T. (1988) *Numerical recipes in C, the art of scientific computing*, Cambridge University Press, Cambridge.

Shaka, A. J., Barker, P. B., & Freeman, R. J. (1985) *J. Magn. Reson. 64*, 547−552.

Shaka, A. J., Lee, C. J., & Pines, A. (1988) *J. Magn. Reson. 77*, 274−293.

Sklenar, V., Piotto, M., Leppik, R., & Saudek, V. (1993) *J. Magn. Reson. A 102*, 241−245.

Spurlino, J. C., Smallwood, A. M., Carlto, D. D., Banks, T. M., Vavra, K. J., Johnson, J. S., Cook, E. R., Falvo, J., Wahl, R. C., Pulvino, T. A., Wendolski, J. J., & Smith, D. L. (1994) *Proteins: Struct., Funct., Genet. 19*, 98−109.

Stams, T., Spurlino, J. C., Smith, D. L., Wahl, R. C., Ho, T. F., Qoronfleh, M. W., Banks, T. M., & Rubin, B. (1994) *Nat. Struct. Biol. 1*, 119−123.

States, D. J., Haberkorn, R. A., & Ruben, D. J. (1982) *J. Magn. Reson. 48*, 286−292.

Van Doren, S. R., Kurochkin, A. V., Ye, Q.-Z., Johnson, L. L., Hupe, D. J., & Zuiderweg, E. R. P. (1993) *Biochemistry 32*, 13109−13122.

Van Doren, S. R., Kurochkin, A. V., Hu, W. D., Ye, Q.-Z., Johnson, L. L., Hupe, D. J., & Zuiderweg, E. R. P. (1995) *Protein Sci. 4*, 2487−2498.

Walther, S. E., & Denhardt, D. T. (1997) *Cell Growth Differ. 7*, 1579−1588.

Will, H., Atkinson, S. J., Butler, G. S., Smith, B., & Murphy, G. (1996) *J. Biol. Chem. 271*, 17119−17123.

Willenbrock, F., Crabbe, T., Slocombe, P. M., Sutton, C. W., Docherty, A. J. P., Cockett, M. I., O'Shea, M., Brocklehurst, K., Phillips, I. R., & Murphy, G. (1993) *Biochemistry 32*, 4330−4337.

Williamson, R. A., Marston, F. A. O., Angal, S., Koklitis, P., Panico, M., Morris, H. R., Carne, A. F., Smith, B. J., Harris, T. J. R., & Freedman, R. B. (1990) *Biochem. J. 268*, 267−274.

Williamson, R. A., Smith, B. J., Angal, S., & Freedman, R. B. (1993) *Biochim. Biophys. Acta 1203*, 147−154.

Williamson, R. A., Martorell, G., Carr, M. D., Murphy, G., Docherty, A. J. P., Freedman, R. B., & Feeney, J. (1994) *Biochemistry 33*, 11745−11759.

Williamson, R. A., Natalia, D., Gee, C. K., Murphy, G., Carr, M. D., & Freedman, R. B. (1996) *Eur. J. Biochem. 241*, 476−483.

Wishart, D. S., Sykes, B. D., & Richards, F. M. (1991) *J. Mol. Biol. 222*, 311−333.

Woessner, J. F. (1991) *FASEB J. 5*, 2145−2154.

BI9712091